Mobility and the Distribution of Free Volume in Epoxy Network by Photochromic Labeling and Probe Studies

Wei-Ching Yu and Chong Sook Paik Sung*

Institute of Materials Science, Department of Chemistry, University of Connecticut, Storrs, Connecticut 06268. *Received June 25, 1987*

ABSTRACT: Mobility and the free volume environments at different sites of a growing epoxy–diamine network (DGEBA–DDS) have been evaluated by site-specific labeling with azobenzene chromophores. The sites investigated are the cross-linker and the chain end or the dangling chain in the network. We also investigated the free volume of the least constrained region between the network chains by using a free probe not attached to the network. Trans → cis photoisomerization kinetics of the two labels and the free probe were studied as a function of increasing cure at 160 °C. Throughout the cure process, the photoisomerization kinetics can be analyzed by two rate processes, suggesting two distinct environments. We assume the fraction of the rapid process (α) to be the cumulative area above the critical size in the distribution of free volume. At the cross-link site, the fast fraction decreases sharply when the matrix approaches the gel point, after which no photoisomerization occurs. At the dangling chain, α decreases more slowly up to gelation but even more slowly after gelation when plotted against the T_g of the matrix. For the probe molecule, a similar trend in α values through gelation is obtained, but with the slowest rate of change. For all the network sites and the probe studied, the rate of decrease in α before gelation is greater than after gelation. This trend is predicted from the overall volume contraction based on volume changes as a function of cure. Assuming the rotation as the photoisomerization mechanism, the estimates of the maximum critical size for the labels and the probe before and after cure have been made. Using such estimates, we obtain cumulative distribution curves of free volume, from which the average free volume size is found to be reduced from about 8 Å in radius before cure to about 6.5 Å in radius after cure.

Introduction

Recently, we reported that the free volume and its size distribution can be probed by the use of photochromic labels.[1,2] Analyses of the photoisomerization behavior of photochromic labels allows such processes as physical aging, plasticization, and volume dilation due to glassy deformation to be sensitively monitored. While a single rate can characterize the photoisomerization of the attached label in dilue solution, we had to invoke at least two rates for the solid films. The rate in dilute solution is similar to the fast rate in the solid film, with the slow rate at least one hundred times slower than the fast one. Physical aging reduces the fraction (α) of the fast process while it increases with temperature, plasticization, or glassy deformation. This fast fraction has been interpreted as the cumulative area above the critical size for the particular label in the size distribution curve of free volume, with the assumption that a critical size free volume is required in the immediate vicinity of the label for photoisomerization.

Using such labels we evaluated free volume environments at different sites along the polystyrene chain.[2b] We also investigated the free volume of the least constrained regions between the chains by the use of the free probe not attached to the polymer molecule. It was found that at any given aging time, the magnitude of the fast reaction was the greatest for the free probe, followed by chain ends, side groups, and chain center in decreasing order. The Robertson–Simha–Curro theory[3] has been used to compute the populations of regions having a greater than critical amount of free volume. Except for the recovery data at 30 °C below T_g, the computed fit to the data is quite satisfactory.

In this study, we use reactive labels and free probe molecule in an epoxy–diamine network to determine the distribution of free volume as a function of cure. As cure proceeds, it is well-known that there is overall volume contraction with a subsequent increase in density,[4] even though some anomalous density behavior has been reported.[5] In this study, we are particularly interested in characterizing the distribution of free volume as cure proceeds, specifically in the vicinity of the cross-linker and the dangling chain. We will compare these sites with the least constrained region between the network chains by the use of a free probe unattached to the growing network.

In recent years, several physical techniques have been applied to probe the structure, mobility, and the free volume in cured epoxy network. Wu and Bauer have used neutron scattering to elucidate epoxy network structure,[6] namely, the distance between cross-links, the average molecular weight, its distribution, and network heterogeneity. Sandreczki and Brown used ESR probes to study mobility in four epoxy networks which had different cross-link density.[7] They were able to fit the mobility above the glass transition temperature based on the WLF equation, but below T_g they were not able to get any quantitative data on the mobile fraction. They later extended their ESR work by using some labels and probes to investigate mobility in swollen, cured epoxy.[8] They found that mobility was greatest for the probe, followed by the end label and the bridging label. Jean et al.[9] used positron annihilation studies to estimate the average free volume sizes in the same cured epoxies studied by Sandreczki and Brown. By using a calibration curve to correlate the free volume sizes and the lifetime of the triplet positronium atom, they estimated the average free volume sizes to vary from 3.6 to 7.5 Å in diameter, over a wide range of temperatures and cross-link densities.

As far as we are aware, this is the first study where the mobility and the distribution of the free volume are continuously monitored from the unreacted epoxide–diamine mixture through the cure transformations of gelation and vitrification. For labels, we use two types: one, a reactive diamine, *p,p'*-diaminoazobenzene (DAA), and the other, a reactive monoamine, *p*-aminoazobenzene (AA). In order to closely match the reactivities of these labels, we use *p,p'*-diaminodiphenyl sulfone (DDS) as the curing agent with a diepoxide, diglycidyl ether of bisphenol A (DGEBA). As shown in our previous studies,[10] DAA gets incorporated into the network as a cross-linker, even though it reacts slightly faster than DDS. On the other hand, AA is in-

0024-9297/88/2221-0365$01.50/0

Chart I
Chemical Structures of the Labels, Probe, and Epoxy Matrix Resins

Labels

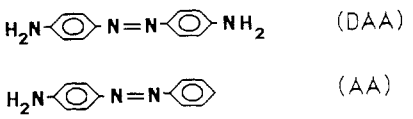

Probe

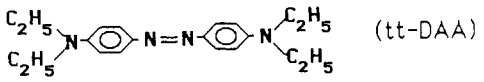

Epoxy Matrix Resins

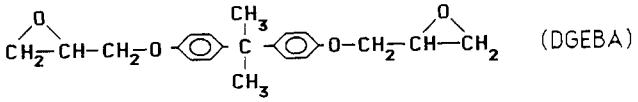

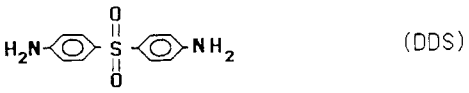

corporated as the chain ends at early stages of cure but ends up as dangling chains at later stages of cure. For the free probe we use a derivative of DAA whose four amine hydrogens are fully substituted with ethyl groups, here designated tt-DAA. This probe will no longer react with DGEBA because the amine groups are fully reacted. The chemical structures of the labels, the probe, and the epoxy components used are shown in Chart I.

Another epoxy matrix, diglycidyl ether of butanediol (DGEB) cured with DDS would provide a medium where mobility could be followed up to almost complete cure (95%), because of a lower T_g and the lack of vitrification at the cure temperatures.[10a] Unfortunately, the thermal cis → trans isomerization is catalyzed in DGEB, making accurate analyses of trans → cis photoisomerization difficult at room temperature. For this reason, we only studied DGEBA–DDS epoxy in this study.

Experimental Section

Materials. *p,p'*-Diaminoazobenzene (DAA) was recrystallized from toluene and acetone. *p*-Aminoazobenzene was used as received from Eastman Kodak Chemical Co. Diglycidyl ether of bisphenol A (DGEBA) was recrystallized from MEK solution by seeding it with DGEBA crystal and leaving it in the freezer at −20 °C for 2 weeks. *N,N'*-diethyl-*p,p'*-diaminoazobenzene (tt-DAA) was synthesized by reacting DAA with excess ethyl iodide and separating the products with a series of extractions by a method described by Fuguitt et al.[11] The structure of tt-DAA was confirmed by NMR, IR, and UV–vis spectroscopy. The absorption maximum in phenyl glycidyl ether (PGE) of tt-DAA was 470 nm, close to the value reported on the model compound between DAA and PGE.[10a]

Photoisomerization Studies. A small amount of the labels (DAA or AA) (0.16%) or the probe molecule (tt-DAA) (0.10%) was mixed to a stoichiometric mixture of DGEBA–DDS epoxy, by heating to 100 °C for 5 min. Two circular quartz plates were clamped together with two thin Mylar films (1.5 mil) on the edges leaving a center space for sample. The clamped quartz plates with Mylar spacers were dipped into epoxy heated to 100 °C, and the sample went into the center space by capillary action. UV–visible spectra were measured after curing in an oven at 160 °C for a specific time and cooling the sample to room temperature, using a Perkin-Elmer diode-array system with a Model 7500 data

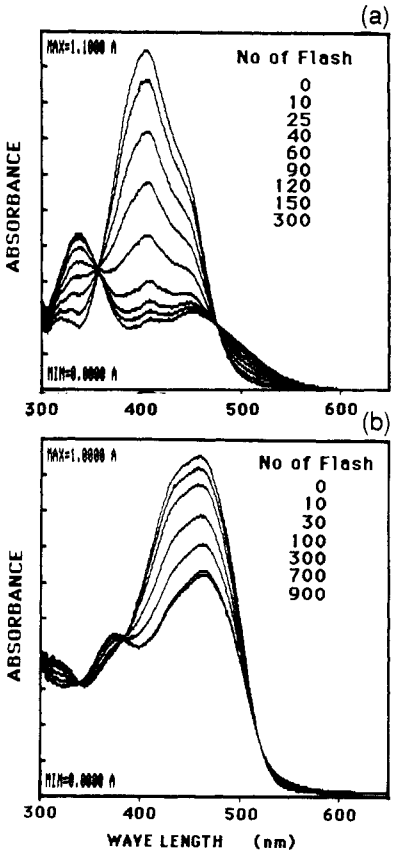

Figure 1. UV–vis absorption spectra of DAA (a) and tt-DAA (b) in dilute phenyl glycidyl ether solution as a function of the number of irradiating flashes at 25 °C.

station. The optical density at λ_{max} of the label or the probe was in the range of 0.7–1.0. A PRA flash lamp (Model 6100A) was used to irradiate the sample for trans → cis photoisomerization. The irradiating light sources were selected to be near the λ_{max} of the cured label or the probe by using a narrow band interference filter.

The T_g measurements of samples were conducted with a Perkin-Elmer DSC-2. Small sample quantities (10–15 mg) were placed in the sealed aluminum pans and run at a heating rate of 10 °C/min after curing in an oven at 160 °C for different times.

Results and Discussion

(A) Photoisomerization in a Low Viscosity Solvent. Before the labels and the probe were studied in epoxy network as a function of cure, we characterized their photoisomerization behavior in a low viscosity solvent. We chose phenyl glycidyl ether (PGE) as the solvent in order to simulate the epoxy matrix as closely as possible. Figure 1a shows the UV–visible spectra in the 300–600 nm range, due to the photoisomerization of DAA. The top curve in Figure 1a corresponds to the spectrum before irradiation, representing 100% trans isomer. The absorption maximum occurs at 410 nm, corresponding to the $\pi \rightarrow \pi^*$ transition of the trans azo bond in DAA. As the solution is irradiated at 400 nm by successive flashes from the flash lamp, the absorption at 410 nm decreases while the absorption at 337 nm due to the $\pi \rightarrow \pi^*$ transition of the cis isomer increases. The $n \rightarrow \pi^*$ transition at 455 nm becomes more obvious with extensive irradiation since this peak is stronger in the cis isomer. Thus, after 300 flashes, the absorbance at 410 nm is about 0.2, including the contribution from two cis peaks at 337 and 455 nm. After subtracting the contribution due to cis isomer, we estimate that the trans content at the photostationary state is about 10%, which is in agreement with other azo labels in dilute solution.[1,2]

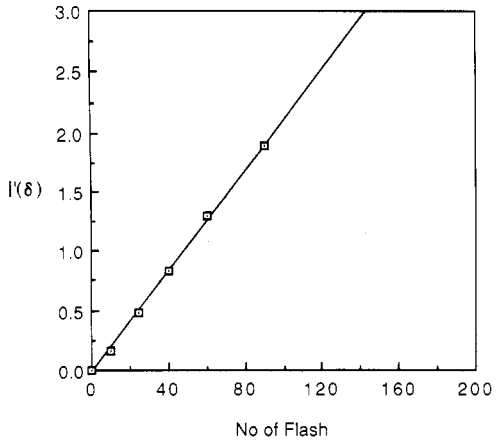

Figure 2. Kinetic plot of photoisomerization of DAA in dilute phenyl glycidyl ether solution (y_∞ is assumed to be 90%).

Table I
Trans → Cis Photoisomerization Rate Constant and the Relative Fluorescence Quantum Yield of DAA, AA, and tt-DAA in Phenyl Glycidyl Ether

	rel photoisom rate	rel ϕ_f
DAA	0.022	1
AA	0.020	1
tt-DAA	0.021 (0.38[a])	1400

[a] Assuming 60% cis content at the photostationary state.

The kinetics of photochemical trans → cis isomerization were followed by monitoring optical density at 410 nm for the trans isomer and analyzed with eq 1, which is a good

$$I(\delta) \simeq \left(1 + \frac{D_\infty}{2} + \frac{D_\infty^2}{12}\right) \ln|\delta| - \left(\frac{1}{2} + \frac{D_\infty}{6}\right)\delta + \frac{\delta^2}{24} = -At + \text{const} \quad (1)$$

approximation of the solution of the reversible photochemical rate equation when the thermal isomerization is negligible, where $\delta = D_\infty - D$ and D_∞ and D are, respectively, optical densities at the photostationary state ($D_\infty = 0.9D_0$ in this case) and at time t (or after t flashes). Figure 2 shows a plot of $I'(\delta)$ versus the number of flashes where $I'(\delta)$ is $I(\delta)$ minus the intercept before any flash. Due to the complication on the absorption from the cis isomer at high conversion, we only plotted the first five points where correction on the optical density was considered unnecessary. The slope (A) of such a plot as in Figure 2 is proportional to the quantum yield of photoisomerization (ϕ_t) since

$$A = I_0\phi_t\epsilon_t/y_\infty$$

where I_0 is the irradiation intensity, ϵ_t is the molar extinction coefficient of the trans isomer, and y_∞ is the fraction of the cis isomer at the photostationary state. In this study we did not attempt to measure absolute ϕ_t but used the slope as the relative quantum yield or the relative rate of photoisomerization. The slope from Figure 2 for DAA data was calculated to be 0.022.

The photoisomerization behavior of AA in PGE was found to be similar to DAA. The slope of the plot of $I'(\delta)$ versus the number of flashes was determined to be 0.020, which is same as that of DAA in PGE within experimental error (see Table I).

The probe molecule, tt-DAA, showed more than one thousand times stronger fluorescence than DAA showed.[10,11] Therefore, it was of great interest to see if the enhanced fluorescence occurred at the expense of the photoisomerization quantum yield, as is the case in

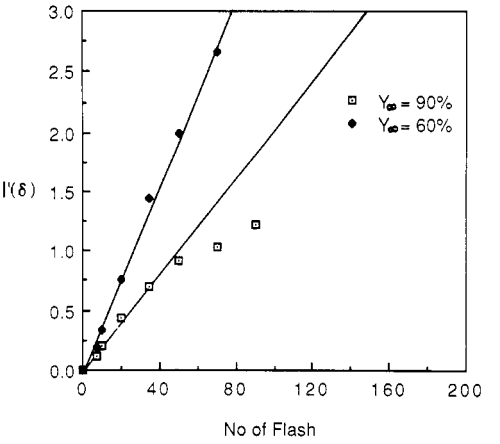

Figure 3. Kinetic plot of photoisomerization of tt-DAA in dilute phenyl glycidyl ether solution.

trans-stilbene and some stilbene derivatives.[12] The photoisomerization behavior of the probe molecule, tt-DAA, is illustrated in Figure 1b, as a function of irradiation from a flash lamp centered around 460 nm. The top curve, corresponding to 100% trans isomer, shows the absorption maximum at 470 nm. With increasing irradiation flashes, we note the decrease of the peak at 470 nm and the emergence of the peak at 380 nm, due to the cis isomer of the probe. The decrease of the peak at 470 nm is not as great as the decrease of the 410-nm peak for DAA (see Figure 1a). This is due to the fact that underneath this 470-nm peak there is a hidden cis absorption peak due to the n → π* transition. In order to minimize complications due to these opposing effects on the optical density at 470 nm, we have only used the first five curves of Figure 1b for the photoisomerization kinetic analysis using eq 1. As for the cis content at the photostationary state, we have assumed two values, 90% or 60% in the calculation for eq 1, since we cannot independently determine its value due to the overlap between the n → π* and π → π* transitions. Figure 3 shows the plot of $I'(\delta)$ versus the number of flashes for the probe molecule in PGE. When the *cis* content at the photostationary state, y_∞ was assumed to be 60%, the slope was 0.038 while it was 0.021 when y_∞ is assumed to be 90%. These values of the slope are similar to the value for the DAA label in PGE, especially when y_∞ is 90%.

Clearly, the rate of photoisomerization is of a similar order of magnitude for both DAA and tt-DAA. Thus, the effect of ethyl substitution on both nitrogen atoms of DAA has little effect on the quantum yield of photoisomerization in spite of the large increase in fluorescence quantum yield. This observation is consistent with the study by Gegiou et al.[13] where no significant effect was observed on other substituted azobenzenes. While the substituted azobenzenes studied by Gegiou et al. did not result in fluorescence enhancement, tt-DAA exhibited strikingly high fluorescence in comparison to DAA[10,11] as summarized in Table I. Apparently, in DAA and tt-DAA, fluorescence does not compete directly with isomerization, in contrast to the behavior of stilbene and some stilbene derivatives where fluorescence is the main competing process for photoisomerization.[12] As mentioned earlier, *N*-alkyl substitution on DAA leads to the red shift of π → π* transition to be near the n → π* transition. Bisle et al. attributed the observed fluorescence due to the coupling of n → π* and π → π* transitions caused by such red shifts in *N*-alkyl-substituted amino- and diaminoazobenzenes.[14] Nevertheless, the exact photochemical and photophysical pathways and mechanisms of tt-DAA is of great interest and deserves a thorough investigation.

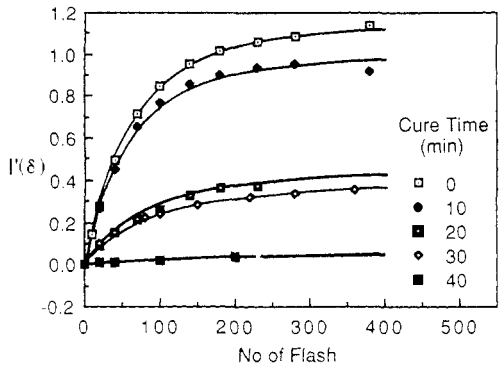

Figure 4. Kinetic plot of photoisomerization of DAA in epoxy matrix at 25 °C, following cure at 160 °C.

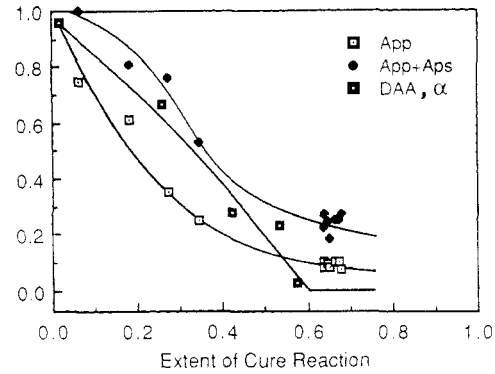

Figure 5. Comparison of the fast photoisomerization fraction, α, for DAA in epoxy matrix with the cure composition of A_{pp} and $A_{pp} + A_{ps}$ as a function of extent of cure reaction.

(B) Photoisomerization in Epoxy Network. DAA (Label) in DGEBA–DDS Epoxy. The photoisomerization behavior of a small amount of DAA label in a stoichiometric mixture of DGEBA–DDS epoxy was studied at room temperature following cure at 160 °C. We monitored photoisomerization throughout the cure with the irradiation centered around the absorption maximum, which changes from 410 to 470 nm. As shown in Figure 4, the photoisomerization kinetic plots of $I'(\delta)$ versus the number of flashes are strongly curved, especially at longer cure times. This tendency is in direct contrast to the linear plot as shown in Figure 2, when DAA is in a low viscosity solvent, but similar to the behavior of azo labels in the glassy state.[1,2] When the plot is non-linear, we have to invoke at least two rate processes to fit the curves, as in eq 2, where k_1 characterizes the fast process, k_2 characterizes the slow process, and α is the fraction characterized by the fast process. Table II summarizes the photoisomerization kinetic parameters, k_1, k_2, and α calculated from Figure 4, based on eq 2. We can note two trends from the results summarized in Table II. First, the values of k_1 and k_2 are in the same order of magnitude, as a function of increasing cure time. Secondly, the fraction of fast photoisomerizable species, α, decreases drastically with cure time especially after 30 min, which corresponded to about 60% reaction of DAA.[10] This behavior is more clearly illustrated in Figure 5 where α is plotted against the extent of reaction of the matrix epoxy (ξ_b). The extent of reaction was obtained by IR monitoring of the disappearance of epoxide peak at 915 cm^{-1}, corrected with the absorption at 1184 cm^{-1} due to C–C stretching of the bridge carbon atom in DGEBA,[10] according to eq 3. The middle line in

$$e^{-I(\delta)} = \alpha e^{-k_1 t} + (1 - \alpha)e^{-k_2 t} \quad (2)$$

$$\xi_b = \frac{A_{915cm^{-1}}(t)}{A_{1184cm^{-1}}(t)} \frac{A_{1184cm^{-1}}(0)}{A_{915cm^{-1}}(0)} \quad (3)$$

Table II
Trans → Cis Photoisomerization Kinetic Parameters for DAA, ttDAA, and AA in Epoxy Matrix as a Function of Cure at 160 °C

cure time, min	$10^{-2}k_1$	$10^{-4}k_2$	α
	DAA		
0	1.41	4.93	0.96
10	1.67	3.87	0.67
20	1.67	3.33	0.27
30	1.99	2.80	0.23
40			0.03
	tt-DAA		
0	4.11	0.85	0.48
10	4.70	0.80	0.50
20	4.70	0.80	0.47
30	2.87	0.80	0.46
40	2.01	0.90	0.41
60	2.42	0.74	0.37
100	2.88	0.45	0.33
210	3.57	0.39	0.32
	AA		
0	0.53	12.30	0.98
10	0.54	9.96	0.89
20	0.65	6.90	0.84
30	0.96	6.13	0.83
60	1.27	6.13	0.76
400	1.67	4.21	0.69

Figure 5 represents the experimental data, which show a drastic decrease in the photoisomerizable fraction well before gelation (occurring at about 56% reaction in this matrix), followed by no photoisomerization in the post-gelation period. In spite of the fact that DAA reacts somewhat faster than the curing agent, DDS, the gelation of the matrix seems to occur at close to 60% of the DAA reaction when cured at 160 °C.[10] Since the entire cure was carried out at 160 °C, we use the terms for the gelation of the matrix and for that monitored by the DAA interchangeably.

It is useful to estimate which cure species are able to isomerize as cure proceeds. As a first approximation, we may expect that only some fractions of unreacted DAA and/or dimer (DAA reacted with one epoxide) can photoisomerize since branched species or the cross-linker are not likely to have enough mobility in this rigid, glassy epoxy matrix. It is known, however, that even the cross-linker can photoisomerize substantially as long as it is in a rubbery matrix.[15] Therefore we plot two curves in Figure 5, one corresponding to the sum of the unreacted DAA (A_{pp}) and the dimer (A_{ps}), and one corresponding to the unreacted DAA alone. These curves were obtained by the deconvolution of the UV–vis spectra as a function of cure.[10] In this plot we observe that the experimental data (middle line) falls between the A_{pp} curve and that representing the sum of A_{pp} (unreacted DAA) and A_{ps} (dimer or chain end). This behavior can be explained by considering the glass transition temperature of the matrix as a function of the cure extent, obtained by differential scanning calorimetry for a stoichiometric mixture of DGEBA–DDS cured at 160 °C. As seen in Figure 6, the T_g of the freshly mixed matrix is near −6 °C. As cure proceeds, the T_g rises sharply, especially after gelation, toward 215 °C which is the maximum T_g obtainable for this matrix.[16] Figure 6 shows that the matrix was in the rubbery state up to 20% of conversion at room temperature, which was the temperature for measuring mobility. However, beyond that, the matrix approaches glassy state at room temperature. This transition from the rubbery state to the glassy state at the measurement temperature is apparently responsible for the observed behavior in Figure 5. Such limited mobility as manifested in the photoisomerization behavior of azo

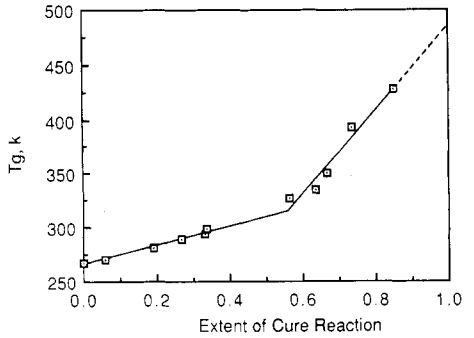

Figure 6. Changes in the glass transition temperature of epoxy matrix as a function of extent of cure reaction.

probes has been observed in other studies in polystyrene glass[17] as well as in our previous study.[2]

Beyond gelation, the matrix T_g rises even faster than before gelation due to the increasing number of cross-links. In fact, the changes in T_g can be represented by two linear lines in this matrix whose point of intersection coincides with gelation point. Recently, Cizmecioglu et al.[4a] observed a similar behavior of T_g in a tetrafunctional epoxy cured with DDS. Therefore the photoisomerization measurement temperature is far below the matrix T_g after gelation. This situation combined with the fact that the matrix becomes tightly cross-linked must contribute to the apparent lack of mobility of DAA after gelation.

AA (Label) and tt-DAA (Probe) in DGEBA–DDS Epoxy. The photoisomerization behavior of AA label and tt-DAA probe in this epoxy matrix as a function of cure at 160 °C also deviates from linearity when $I'(\delta)$ is plotted against the number of flashes. Equation 2 has been used to fit the curves with two rate constants. Table II summarizes the kinetic parameters as well as the fast fraction α for AA and tt-DAA in the last two columns. A comparison of these last two columns with the analogous parameters for DAA in the epoxy matrix will indicate two trends: First, the values of κ_1 and κ_2 are similar in order of magnitude, except for the values of k_2 for tt-DAA, which are about 1 order of magnitude smaller. We will comment on this difference in the last section of this paper. Secondly, the values of α for AA and tt-DAA do not decrease as sharply as for DAA as a function of cure. This trend is more clearly illustrated in Figure 7, where the fast fraction α is plotted against the glass transition temperature of the epoxy matrix. We chose to use T_g as the abscissa rather than the extent of reaction because we would like to discuss these results from the predicted relation between the total volume and the T_g of the matrix. We will elaborate on this point in the next section.

In contrast to the sharply decreasing α for DAA, α for AA decreases slowly up to the gel point corresponding to the T_g of about 307 K (see Figure 6 for the location of T_g at the gel point). Even after gelation, α for AA remains quite large (~70%). For tt-DAA, the α value starts out only as 0.5 in freshly mixed resin, but its decrease up to the gel point is slower than AA. Like AA, α for tt-DAA after gelation decreases even more slowly so that its value corresponding to the T_g of 440 K (extent of cure about 85%) is still 35%. The lower α value for tt-DAA can be explained by the different size critical free volume required for the two. The probe molecule, tt-DAA will require a larger size free volume for photoisomerization regardless of which photoisomerization mechanism (rotation versus inversion) is invoked, due to the bulky ethyl groups on the amine nitrogens, which are absent in AA. Furthermore, the critical size free volume for AA is not going to increase even after being attached to the epoxy matrix since AA will be a dangling chain with only one end of the molecule attached. It can be either rotated or inverted by involving only the unattached half of the molecule. The estimates of such critical size free volumes and how they could be used to obtain the distribution of free volume before and after cure will be discussed in a later section of this paper.

(C) Comparison of Experiment with Predicted Volume Contraction. As shown in Figure 7a, the experimentally obtained fraction of the fast photoisomerization process (α) exhibits a break at gelation. Under the assumption that these α values represent the cumulative area above the critical size for the particular label or probe in the size distribution curve of free volume, these trends clearly indicate the skewing of free volume size distribution toward smaller sizes as cure proceeds. This is expected, at least qualitatively, from the volume contraction accompanying cure reactions.

In our physical aging studies, we were able to compare the experimentally measured α values with the computed α values predicted from the Robertson–Simha–Curro theory.[3] In the curing of an epoxy network, no theory is yet available to predict the changes in free volume sizes, so we cannot directly compare experimental α values from a theoretical α value. Instead, we will attempt to compare the experimental values with the predicted volume contraction in this section.

In order to carry out the above objective, we need to estimate total volume and the specific volume as a function of extent of cure. As a first approximation, we assume the additivity of molar volumes of each functional group. Then for a stoichiometric mixture of DGEBA and DDS, the initial volume (V_0) at 25 °C can be estimated as follows

$$V_0 = 2\,(\text{moles}) \times 2\,(\text{epoxide})\, V_E + 1\,(\text{mole}) \times 2V_a + \sum V_R \quad (4)$$

where V_E, V_a, and $\sum V_R$ correspond to the molar volume of epoxide (21.8 cm^3/mol)[4a] of the amine (19.2 cm^3/mol)[4a] and of the contribution by all other groups (562.4 cm^3/mol).[18]

Therefore, V_0 is estimated to be 688 cm^3 for a stoichiometric mixture of 2 mol of DGEBA and 1 mol of DDS. The weight of such a stoichiometric mixture is 928 g, which would make the specific volume of unreacted mixture, ν_0, equal to 0.741 (= 688/928). After a certain extent of cure (ξ_b), the volume (V) can be estimated by assuming the two main reactions to be the reactions of the epoxide with the primary amine and the secondary amine. Each of these reactions results in the average volume contraction (ΔV) of 25.9 cm^3/mol because of the formation of the new chemical bond.[4a] Therefore, we can write the volume as in eq 5, according to a procedure described by Cizmecioglu et al.[4a]

$$V = V_0 + 4\Delta V \xi_b \quad (5)$$

By substituting the values of V_0 and ΔV in eq 5, we obtain eq 6.

$$V = 688 - 103.6\xi_b \quad (6)$$

After dividing by the total weight of the stoichiometric mixture (928), we obtain eq 7, to relate the specific volume to the extent of reaction. Now, we need to correlate the

$$\nu = 0.741 - 0.112\xi_b \quad (7)$$

specific volume to the T_g of the matrix, in order to compare with the experimental data (Figure 7). From Figure 6, we can obtain the following empirical relations between T_g and the extent of reaction (ξ_b):

$$\xi_b = (T_g - 267)/90.3 \quad \text{before gelation} \quad (8)$$

$$\xi_b = (T_g - 112.4)/366.6 \quad \text{after gelation} \quad (9)$$

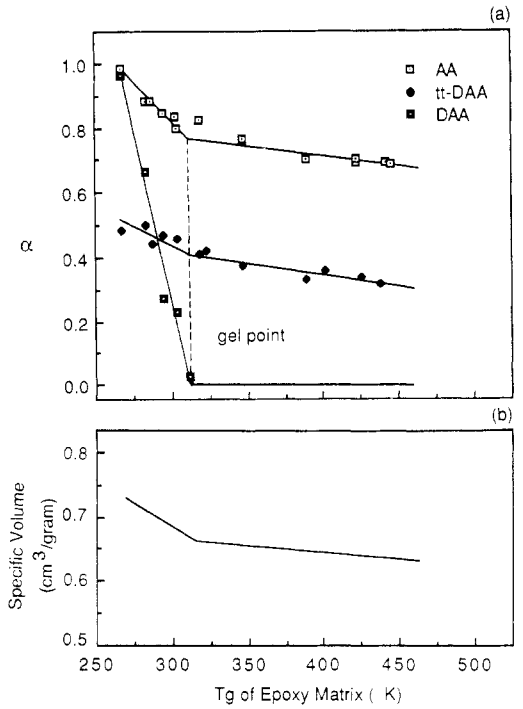

Figure 7. Changes in the fast photoisomerization fraction, α, for the labels and probe (a) and in the estimated specific volume (b) as a function of the glass transition temperature of the epoxy matrix.

Substitution of eq 8 and 9 in eq 7 will result in the following equations:

$$\nu = 1.072 - 0.00124T_g \quad \text{before gelation} \quad (10)$$

$$\nu = 0.775 - 0.00031T_g \quad \text{after gelation} \quad (11)$$

Figure 7b provides the plot of specific volume versus the T_g of the matrix based on eq 10 and 11. This figure not only predicts a break at the gel point but also a greater slope before gelation than after the gelation. This behavior is consistent with a trend observed in the experimental data for all the labels and probe. Therefore, we may conclude that the faster rate of volume contraction before gelation (as compared to the post-gelation period) leads to the faster loss of the mobile fraction. However, as manifested in the different slopes of α versus T_g for DAA (cross-linker), AA (dangling chain), and tt-DAA (free probe), the overall volume contraction obviously affects the free volume environment of each site differently.

Equation 7 can be used to estimate the density of the epoxy since it is the reciprocal of the specific volume. The density is estimated to be 1.349 before cure and 1.589 g/cm^3 after 85% cure. These density values are too high in comparison to the actual reported values in the DGEBA–DDS epoxy,[16] probably due to the approximations inherent in the molar volume calculation of the functional groups. However, the trends of volume contraction and the different slope before and after gelation as in Figure 7b are expected to be valid. Recent data by pressure dilatometer provide direct support of these expectations: When Choy and Plazak measured specific volume of a DGEBA resin cured with DDS,[19] they showed that the specific volume decrease rapidly initially, followed by a slow decreases as a function of cure time at 150 °C cure.

(D) Distribution of Free Volume before and after Cure. With the assumption that the two-process kinetic behavior of photoisomerization is a reflection of the distribution of free volume in an epoxy matrix, we can use the fraction of the fast process, α to indicate the free volume size distribution in the vicinity of a site in the growing epoxy network or in between the network chains. In other words, the fast fraction is equivalent to the cumulative area under the free volume size distribution curve above the critical size necessary for each label of the probe. Before cure, neither the labels nor the free probe is reacted. Thus, the fraction of the fast process α will be determined by the different critical size requirement of the labels or the probe, providing the distribution of free volume sizes before cure.

Table III
Estimated Critical Radius of DAA, AA, and tt-DAA before and after Cure in Epoxy Matrix

		critical radius, Å	
		before cure	after cure
DAA	cross-linker	6.2	10.8
AA	dangling chain	4.5	4.5
tt-DAA	free probe	8.2	8.2

Table III lists the estimates of the radius of the critical size free volume for the labels and the probe before and after cure. These values have been obtained by assuming rotation as the photoisomerization mechanism. Since the alternate mechanism, inversion, would require less volume change, these values would represent the maximum estimates. It is worth noting that Victor and Torkelson take somewhat different approaches to estimate the critical volume necessary for the photoisomerization.[20] They estimate the extra volume needed for photoisomerization from the volume swept by the van der Waals area, which requires the knowledge of the exact X-ray structure of the dyes used. In view of the controversy still existing on the exact X-ray structure of azobenzene and the absence of such structural determination on DAA and tt-DAA, we chose not to use their method. However, their values are in general lower than our values; for example, they estimate volume with 3-Å radius for azobenzene while we estimate it to have a radius of 4.5 Å.

As seen in Table III, the radius for the AA is smallest, followed by DAA and tt-DAA before cure. This is because AA can photoisomerize by rotating the other half of the molecule, not involving the para amino group. Due to the bulky ethyl groups on both of the nitrogen groups in tt-DAA, its critical radius is greater than DAA. These values were estimated by building a molecular model with the most probable configuration of the amino group on the *p,p'*-positions.

It is reasonable to expect that the critical radius for AA and tt-DAA would remain unchanged throughout the cure process. However, estimation of the critical radius for DAA as cure proceeds is difficult. After extensive cure such that DAA has become a cross-linker, it seems that the photoisomerization would then require the involvement of attached chains, making the critical radius larger. In the rubbery network, a DAA-type cross-link is reported to photoisomerize easily, presumably involving some flexible rubbery parts in view of the availability of the large size free volumes. As a first approximation, we are going to assume that at least the flexible part of DGEBA (CH_2CHCH_2O–) is involved in the photoisomerization of a cross-linked DAA. Under this assumption, the critical radius becomes about 10.8 Å. On the basis of the estimated values listed in Table III and the results of the fast fraction given in Table II, now we can plot α, the cumulative area above the critical size, as a function of the critical size required. Figure 8 illustrates two such curves, one representing the cumulative distribution of free volume before cure and the other for the same after extensive cure. The data used for the latter curve were taken from the last set of data points in Table II, corresponding to 85% cure.

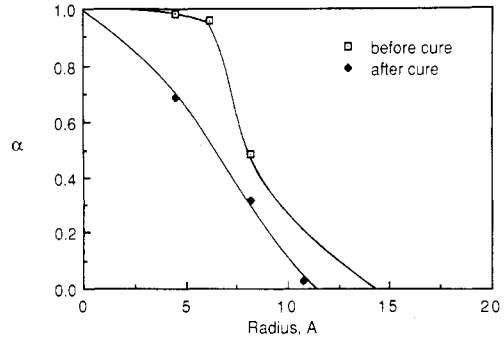

Figure 8. Fast photoisomerization fraction, α, representing cumulative distribution above the critical free volume size as a function of free volume radius, before and after cure.

From Figure 8, almost all the free volume in the uncured state is larger than 6.2 Å° in radius but only about half of it is greater than 8 Å in radius. This is why the α value for tt–DAA is much smaller than that for DAA or AA, since tt-DAA would require a volume about 8.2 Å in radius. We do not have experimental data to predict how the cumulative distribution curve will fall when the radius is greater than 8 Å. Assuming it falls smoothly, as drawn in Figure 8, the average size of free volume before cure is thus estimated to be about 8 Å in radius. On the other hand, after 85% of cure, the cumulative distribution has been significantly shifted toward smaller sizes as illustrated in Figure 8. Now, only 70% of the free volume sizes are greater than 4.5 Å in radius, about 35% are greater than 8 Å, and none is greater than 12.4 Å. Thus the average free volume after extensive cure (85% cure) would be estimated to be 6.5 Å, which is smaller than the average value before cure.

We have shown earlier that the free probe in a glassy polystyrene matrix seems to seek out regions in the bulk with the greatest free volume, rather than sampling the average environment.[2b] This tendency poses a potential problem in the interpretation of the distribution of the free volume in a growing epoxy network, as monitored by the probe molecule (tt-DAA). Before cure, the matrix is a viscous liquid at room temperature with a T_g of −6 °C. Therefore at room temperature, where the mobility is measured, the probe molecule is not expected to seek out regions of greater free volume since the free volume is larger and rapidly redistributed in the liquid state. After extensive cure (85%), the matrix is highly cross-linked. We may speculate that the probe molecule is trapped by the tight cross-links, thus having difficulty seeking out regions of greater free volume. Certainly the probe in an epoxy matrix at 25 °C is much further below its T_g (~175 °C) than the probe in a polystyrene matrix, making the probe diffusion slower. Anyway, the average size and the distribution of free volume after cure were estimated with two assumptions, one that the probe molecule samples the average environment and the other that the mobility at different network sites is determined by the availability of the free volume. In view of the observed mobility of the cross-link in the rubbery network,[15] the second assumption appears to be valid. At this point, however, we do not have direct support for the first assumption.

It is worthwhile to examine the validity of other assumptions made in this study in view of the observed kinetic parameters, k_1 and k_2 as listed in Table II. In the interpretation of the two-process kinetic behavior of photoisomerization, the fast fraction α is assumed to represent the cumulative area in the free volume size distribution curve above the critical size which is a characteristic of each label or probe. This assumption predicts a different value of α but same rate constant for the fast process. The fact that the values of the fast rate constants, k_1, were similar in magnitude for each label or probe throughout the cure process is supportive of this assumption. Furthermore, the values of k_1, in the epoxy matrix, were of the same order of magnitude as the rate constant in dilute solution (Table I), a tendency consistent with the assumption that α represents a liquid-like environment even in solids.

In our previous studies, we assumed that the rate of redistribution of free volume determines the values of the slow rate constants, k_2, in such a way that those free volume environments having smaller than the critical size have to wait until diffusion of additional free volume makes it larger than the critical size.[1] For example, the values of k_2 decrease with the temperature of the matrix with an activation energy of 2.5 kcal/mol because of slower diffusion of free volume. As shown in Table III, tt-DAA requires the largest critical size during the cure process until DAA becomes a cross-linker. Therefore, it would take longer for those smaller free volume environments tt-DAA to reach the required critical size, resulting in smaller values of k_2 for tt-DAA.

Acknowledgment. We acknowledge the financial support of this work by the Army Research Office (Contract No. DAA 29-85-k-0055) and the National Science Foundation, Polymers Program (Grant No. DMR 82-05897). A careful synthesis of the probe molecule, tt-DAA, was carried out by Mr. R. Mathisen. We acknowledge Prof. R. E. Robertson for helpful comments on the manuscript.

Registry No. (DDS)(DGEBA) (copolymer), 61467-24-1; DAA, 538-41-0; AA, 60-09-3; tt-DAA, 3588-91-8.

References and Notes

(1) Lamarre, L.; Sung, C. S. P. *Macromolecules* **1984**, *16*, 1729.
(2) (a) Yu, W. C.,: Sung, C. S. P.; Robertson, R. E. *Bull. Am. Phys. Soc.* **1986**, *31-3*, 260. (b) Yu, W. C.; Sung, C. S. P.; Robertson, R. E. *Macromolecules*, in press.
(3) Robertson, R. E.; Simha, R.; Curro, J. G. *Macromolecules* **1984**, *17*, 911.
(4) (a) Cizmecioglu, M.; Gupta, A.; Fedors, R. F. *J. Appl. Polym. Sci.* **1986**, *32*, 6177. (b) Chang, T. D.; Carr, S. H.; Brittain, J. O. *Polym. Eng. Sci.* **1982**, *22*, 1213.
(5) Enns, J. B.; Gillham, J. K. *J. Appl. Polym. Sci.* **1983**, *28*, 2831.
(6) Wu, W.-L.; Bauer, B. J. *Polymer* **1986**, *27*, 169.
(7) Sandreczki, T. C.; Brown, I. M. *Macromolecules* **1984**, *17*, 1789.
(8) Brown, I. M.; Sandreczki, T. C. *Macromolecules* **1985**, *18*, 2702.
(9) Jean, Y. C.; Sandreczki, T. C.; Ames, D. P. *J. Polym. Sci., Polym. Phys. Ed.* **1986**, *24*, 1247.
(10) (a) Sung, C. S. P.; Pyun, E.; Sun, H.-L. *Macromolecules* **1986**, *19*, 2922. (b) Sung, C. S. P.; Chin, I. J.; Yu, W. C. *Macromolecules* **1985**, *18*, 1510.
(11) Fuguitt, R. E.; Stallcup, W. D.; Hawkins, J. E. *J. Am. Chem. Soc.* **1942**, *64*, 2977.
(12) Saltiel, J.; Charlton, J. L. In *Rearrangements in Ground and Excited States*; deMayo, P., Ed.; Academic: New York, 1980; Vol. 3, p 47.
(13) Gegiou, D.; Muszkat, K. A.; Fisher, E. *J. Am. Chem. Soc.* **1968**, *90*, 3907.
(14) Bisle, H.; Römer, M.; Rau, H. *Ber. Bunsen-Ges. Phys. Chem.* **1976**, *4*, 301.
(15) Stadler, R.; Weber, M. *Polymer* **1986**, *27*, 1254.
(16) Enns, J. B.; Gillham, J. K. *Polymer Characterization*; Craver, C. D., Ed.; Advances in Chemistry 203; American Chemical Society: Washington, DC, 1900.
(17) (a) Priest, W. J.; Sifain, M. M. *J. Polym. Sci., Polym. Chem. Ed.* **1971**, *9*, 3161. (b) Victor, J. G.; Torkelson, J. M. *Polym. Mater. Sci. Eng.* **1986**, *54*(1), 700.
(18) (a) Fedors, R. F. *Polym. Eng. Sci.* **1974**, *14*, 152. (b) Van Krevelen, D. W. Properties of Polymers, 2nd ed.; Elsevier: 1976; Chapter 4.
(19) Choy, I.-C.; Plazek, S. J. *J. Polym. Sci., Polym. Phy. Ed.* **1986**, *24*, 1303.
(20) Victor, J. G.; Torkelson, J. M. *Macromolecules* **1987**, *20*, 2241.